

LASER: Lip Landmark Assisted Speaker Detection for Robustness

Le Thien Phuc Nguyen* Zhuoran Yu* Yong Jae Lee
 University of Wisconsin - Madison
 {plnguyen6, zhuoran.yu}@wisc.edu
 yongjaelee@cs.wisc.edu

Abstract

Active Speaker Detection (ASD) aims to identify speaking individuals in complex visual scenes. While humans can easily detect speech by matching lip movements to audio, current ASD models struggle to establish this correspondence, often misclassifying non-speaking instances when audio and lip movements are unsynchronized. To address this limitation, we propose **Lip landmark Assisted Speaker dEtection for Robustness (LASER)**. Unlike models that rely solely on facial frames, LASER explicitly focuses on lip movements by integrating lip landmarks in training. Specifically, given a face track, LASER extracts frame-level visual features and the 2D coordinates of lip landmarks using a lightweight detector. These coordinates are encoded into dense feature maps, providing spatial and structural information on lip positions. Recognizing that landmark detectors may sometimes fail under challenging conditions (e.g., low resolution, occlusions, extreme angles), we incorporate an auxiliary consistency loss to align predictions from both lip-aware and face-only features, ensuring reliable performance even when lip data is absent. Extensive experiments across multiple datasets show that LASER outperforms state-of-the-art models, especially in scenarios with desynchronized audio and visuals, demonstrating robust performance in real-world video contexts. Code is available at https://github.com/plnguyen2908/LASER_ASD.

1. Introduction

Active Speaker Detection (ASD) [2, 10, 15, 19, 25, 26] is a fundamental task in audiovisual computing which aims to detect if one or more people are speaking in a complex visual scene (usually represented by videos). To effectively accomplish this task, models are not only required to understand the visual scene, extract descriptive visual features of candidate speakers, but also learn to correspond the visual

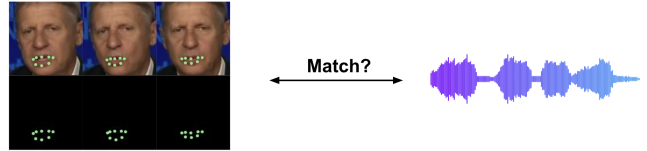


Figure 1. There is a strong correlation between what a person says and how his/her lips move. As humans, we can easily tell if a person is speaking by corresponding the lip movement and the speech. However, existing state-of-the-art active speaker detection methods (e.g., [10, 26]) do not explicitly encode lip movement, and consequently, struggle to establish this correspondence, often misclassifying non-speaking instances when audio and lip movements are unsynchronized.

information to corresponding audio information. Advanced applications in audiovisual computing such as human-robot interaction [11, 22, 24] and multimodal chatbots [8, 23, 27] usually rely on the success of ASD.

How can we, as humans, tell whether a person is speaking? The synchronization of mouth movements with speech is a natural indicator, allowing us to effortlessly perceive when someone is actually speaking [17]. Even a slight delay that desynchronizes audio and visual cues creates discomfort, making it immediately apparent that the person is not truly speaking at that moment. This inherent sensitivity to audiovisual alignment highlights the central role of mouth movement in active speaker detection.

Do existing ASD models function in the same intuitive way, and can they detect when a person is not speaking if the audio and mouth movements are unsynchronized? Unfortunately, based on our analysis, the answer to both questions is no. State-of-the-art ASD models consist of two main phases: (1) visual and audio temporal representation learning, which encodes video and audio streams into sequences of visual and audio embeddings with temporal context, and (2) inter- and intra-person context modeling, which leverages cross-attention to capture long-term temporal dependencies and visual-audio interactions. While current approaches often utilize attention mechanisms to model inter- and intra-person context [1, 2, 5, 19, 26], they still struggle

*equal contribution

to maintain a focus on mouth movement when determining if a person is speaking (Figure 2a). This limitation prevents these models from reliably identifying unsynchronization between audio and visual cues, a key factor in human perception.

While most existing work focuses on improving context modeling, we argue that such limitations stem from the visual features themselves, even before they reach the context modeling module. To address this, we propose **Lip landmark Assisted Speaker dEtection for Robustness (LASER)** to overcome these limitations. The key novelty of LASER lies in the visual temporal representation learning of ASD models: instead of relying on the model to learn audiovisual interactions purely from facial frames, LASER explicitly directs the model’s attention to lip movements by incorporating lip landmarks in training. By guiding the model to focus specifically on lip landmarks over other facial regions (Figure 2b), LASER strengthens the model’s capability to accurately detect active speakers and improves its sensitivity to audiovisual synchronization.

Given a face track¹, LASER extracts frame-level visual feature maps and the 2D coordinates of lips landmarks for each frame of the face track using a lightweight facial landmark detector [16], forming a “lip track” corresponding it. We then encode the landmark coordinates to continuous 2D feature maps matching the spatial dimension of the visual feature maps and combine them to form our visual features that combine the information from the face track and the lip track. Since the lip landmarks come in as 2D coordinates instead of continuous visual feature maps, integrating such discrete coordinates with continuous feature maps poses a challenge. To address this, we design a simple-yet-effective encoding strategy that converts the 2D discrete coordinate information into continuous 2D visual feature maps matching the spatial dimensions of the corresponding visual features (details in Section 3.2). Furthermore, to alleviate the sparsity of these feature maps, we aggregate them into dense feature maps through a 1x1 convolution layer. This way, the lip landmark coordinates are converted to dense feature maps carrying out the information on the position and form of the lip. The combined visual features are passed through the visual temporal network to obtain the final visual representations with temporal context and the representation can then be used by selected ASD models to capture long-term temporal dependencies and integrate the information from multimodal features.

While LASER enhances ASD model performance, we observe that facial landmark detectors may occasionally fail to provide reliable outputs due to issues like low resolution, occlusion, or extreme facial angles. For example, on widely used AVA benchmarks [18], approximately 15% of

face tracks in the test sets lack any landmark detection results. Consequently, missing lip landmarks—resulting in the absence of lip track information—can lead to suboptimal model performance on these test videos. To address this challenge, we introduce an auxiliary consistency loss that aligns predictions made using LASER with those based solely on visual features from the face track. Specifically, for each frame of a face track, we optimize a KL-divergence loss between the predictions obtained with LASER and those based on visual face-frame features alone. This auxiliary loss enables the model to maintain accurate predictions even when the lip track is unavailable, effectively eliminating the dependency on a facial landmark detector at test time.

Contributions. 1) We propose LASER, a novel ASD approach that explicitly directs the model’s attention to lip movements by incorporating lip landmarks in training through effective landmark encoding. 2) We introduce an auxiliary consistency loss during training to address the absence of lip track information at test time, successfully eliminating dependency on facial landmark detectors during inference. 3) Through extensive experiments across multiple datasets and diverse evaluation scenarios, LASER demonstrates stronger performance than state-of-the-art models, particularly in cases where visual frames and audio tracks are unsynchronized, showing robust results in real-world video scenarios.

2. Related Work

Active Speaker Detection (ASD) remains a crucial challenge in audiovisual computing, aiming to determine if a person is speaking within a given video clip. Earlier works, such as those by Saenko et al. [20] and Everingham et al. [7], concentrated on extracting facial features through key facial region localization. Specifically, Everingham et al. [7] localized and cropped facial regions to compute feature descriptors, while Saenko et al. [20] explicitly localized the lip regions to detect speaking activity. While these prior approaches align with our intuition that speaking behavior is intricately linked to lip movements, they fundamentally differ from our method. Instead of relying exclusively on visual features from the lip region, our approach transforms the 2D coordinates of lip landmarks into sparse feature maps. This technique captures more precise and nuanced details of lip motion, enhancing the performance of ASD.

Recent work in ASD primarily focuses on capturing long-term temporal context [1, 2, 10, 15, 19, 25, 26]. To accomplish this, sequence models such as RNNs [13, 15], attention mechanisms [5, 26], or combinations of both [1] are commonly used to integrate visual and audio features, enabling a more robust understanding of speaking behavior

¹A face track is a sequence of cropped images of the same person’s face across consecutive frames in a video stream [18].

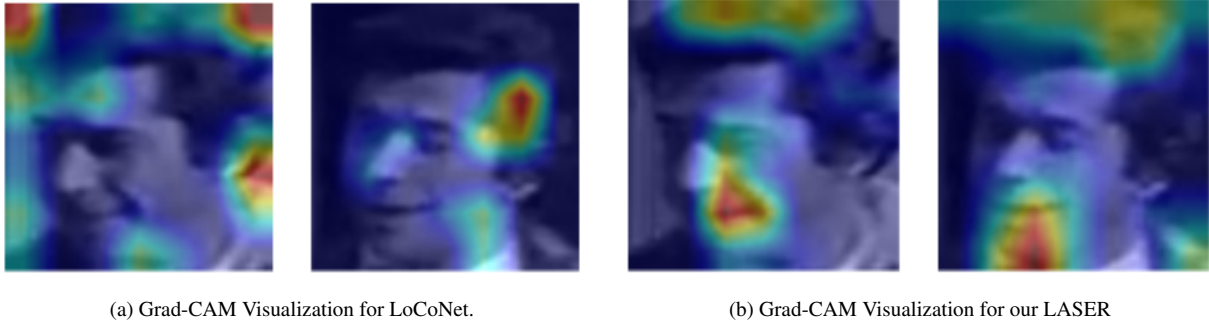


Figure 2. **Qualitative comparison of Grad-Cam [21] visualizations for LoCoNet and our LASER under nonsynchronized audiovisual scenarios.** LoCoNet [26] struggles to accurately predict “not speaking” when visual frames and audio tracks are misaligned, often failing to focus on the lip region when making these predictions. In contrast, our LASER consistently concentrates on the lip area and successfully identifies “not speaking” situations.

over time. Recently, LoCoNet [26] proposes to use self-attention and cross attention for unimodal and multimodal long-term intra-speaker modeling and further uses CNNs for short term inter-speaker modeling. TalkNCE [10] further advances LoCoNet through an auxiliary multimodal contrastive learning objective. In contrast, our approach shifts the focus in ASD by explicitly guiding models to prioritize lip movements in prediction, providing a complementary enhancement to models centered on contextual modeling. As demonstrated in our experiments, training state-of-the-art models LoCoNet with LASER yields improved performance across various evaluation protocols.

3. Approach

In this section, we present the details of our proposed Lip landmark Assisted Speaker dEtection for Robustness (LASER). LASER is a versatile training framework that can be integrated with state-of-the-art ASD models. For this work, we adopt the current state-of-the-art model, LoCoNet [26], as our base model to illustrate LASER’s application without loss of generality. We begin by reviewing the LoCoNet framework (Section 3.1), then describe how we incorporate lip movement guidance into the model (Section 3.2), and finally introduce our consistency loss, which addresses the issue of missing lip landmarks at test time (Section 3.3).

3.1. Preliminaries

The goal of active speaker detection is to classify the speaking activity $Y \in \mathbb{R}^T$ for every frame of a face track $V \in \mathbb{R}^{T \times H \times W}$ conditioned on audio Mel-spectrograms $A \in \mathbb{R}^{4T \times N}$. Here, T is face track’s temporal length, (H, W) is the face crop’s spatial dimension, and N is the number of audio Mel-spectrogram frequency bins.

State-of-the-art ASD models [5, 15, 25, 26] typically consist of two main components: audio-visual encoders and long-term intra-speaker context modeling modules. The

audio-visual encoder includes separate visual and audio encoders, \mathcal{F}_v and \mathcal{F}_a , respectively. The visual encoder \mathcal{F}_v processes visual face tracks to produce visual features $f_v \in \mathbb{R}^{T \times D}$, while the audio encoder \mathcal{F}_a encodes audio spectrograms, generating audio features $f_a \in \mathbb{R}^{T \times C}$, where D and C denote the embedding dimensions for visual and audio features, respectively. f_v and f_a are then concatenated to $f_{av} = \text{concat}(f_v, f_a)$ to form multimodal features and f_{av} is further processed by the context modeling modules \mathcal{G} [5, 15, 25, 26] to aggregate information from both modalities. Typically, \mathcal{G} outputs multimodal features f'_{av} and unimodal features f'_v and f'_a . Linear classifiers, one for each of the three modalities, are then used to process the corresponding features to make final predictions. \mathcal{F} , \mathcal{G} and the linear classifiers are trained end-to-end with the following objective:

$$\mathcal{L}_{\text{asd}} = \lambda_v \cdot \mathcal{L}_v + \lambda_a \cdot \mathcal{L}_a + \lambda_{av} \cdot \mathcal{L}_{av} \quad (1)$$

where \mathcal{L}_{av} is the cross-entropy loss computed between ground-truth labels GT and predictions Y in each frame and L_a and L_v are auxiliary cross-entropy losses computed with ground-truth labels and predictions using the unimodal features f'_v and f'_a , respectively, to avoid \mathcal{G} overly focusing on one modality of features [18].

3.2. Enhanced Representation from Lip Landmark Guidance

While existing work [5, 15, 25, 26] demonstrates competitive performance on the popular AVA-ActiveSpeaker Benchmark [18], our analysis reveals that they still struggle to capture the synchronization between mouth movements and the audio track (Figure 2a). Consequently, they often fail to detect non-speaking scenarios when audio and visual frames are misaligned—an inconsistency that humans intuitively recognize. This limitation highlights the need for enhanced focus on lip-audio synchronization within active speaker detection models (Table 4).

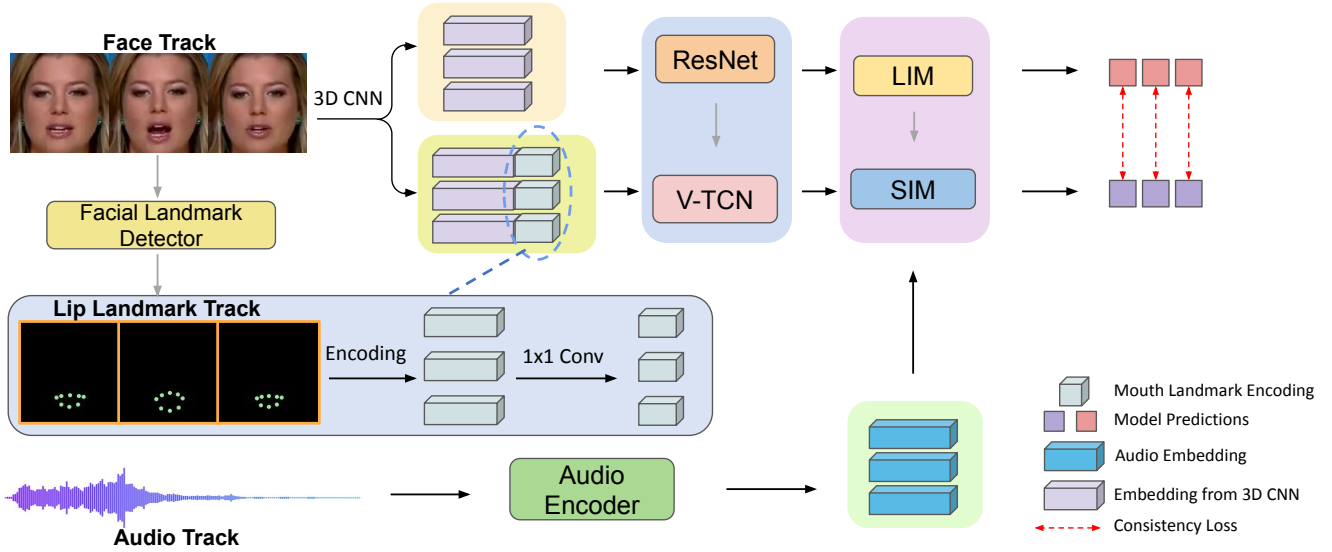


Figure 3. **Illustration of LASER.** Given a face track V , we first obtain a lip landmark track using a facial landmark detector and encode the 2D coordinates of these landmarks into continuous 2D feature maps. These maps are then aggregated through a 1×1 convolution layer. The encoded lip track is concatenated with visual features from a 3D CNN and fed into ResNet and V-TCN to capture a temporal visual representation, which is further processed by context modeling modules to produce the final prediction. For illustration, we use Long-term Intra-speaker Modeling (LIM) and Short-term Inter-speaker Modeling (SIM) from LoCoNet [26]; however, our LASER is not limited to LoCoNet and can be integrated with other models.

We speculate that this limitation stems from the visual features themselves, even before they reach the context modeling module. To address this, we propose LASER, which focuses on enhancing the representations produced by the visual encoder \mathcal{F}_v . By improving these initial visual features, the context modeling module \mathcal{G} can more effectively integrate visual and audio information, ultimately enhancing speaker detection performance.

We adopt the same visual encoder architecture \mathcal{F}_v from prior work [25, 26] where the architecture is composed on a 3D convolution layer, a ResNet-18 [9] backbone, and a video temporal network (V-TCN) [14]. However, unlike prior work which simply forwards visual face tracks to \mathcal{F}_v , we additionally apply a facial landmark detector to the face track and collect a “lip landmark track” M of the corresponding face track. Each lip landmark is represented as 2D coordinates $(x_i, y_i)_{i=0}^K$ where K is the total number of lip landmarks collected.

3.2.1. Lip Landmark Track Encoding

Integrating discrete 2D coordinate information with continuous visual signals during training poses a challenge. To address this, we design a simple-yet-effective encoding function $\mathcal{T}(M)$ that converts the 2D discrete coordinate information to continuous 2D feature maps matching the spatial dimensions of the visual features. Specifically, the encoding process $h = \mathcal{T}(M)$ for each landmark (x_i, y_i) is defined as

follows:

$$h_x^i(u, v) = \begin{cases} x_i/W, & \text{if } u = x_i, v = y_i \\ 0, & \text{if otherwise} \end{cases} \quad (2)$$

$$h_y^i(u, v) = \begin{cases} y_i/H, & \text{if } u = x_i, v = y_i \\ 0, & \text{if otherwise} \end{cases} \quad (3)$$

The encoding process transforms the “lip landmark track” into features $h \in \mathbb{R}^{T \times K \times 2 \times H \times W}$, where K is the total number of lip landmarks, and 2 corresponds to the x and y coordinates. We use the lightweight facial landmark detector from Mediapipe [16] to extract $K = 82$ lip landmarks.

3.2.2. Lip Landmark Track Feature Aggregation

The encoded landmark features are sparse and contain many redundant zero entries, which can hinder optimization during training. To address this, we apply a simple feature aggregation module using 1×1 convolution layers that condense the information from K channels down to S channels, where $S \ll K$. In practice, we find that setting $S = 4$ achieves the best performance, adding only negligible computational overhead. We denote the aggregated landmark feature as $h' \in \mathbb{R}^{T \times S \times 2 \times H \times W}$.

We concatenate the lip landmark track feature h' with the face track visual features output by a 3D convolution

layer and forward the concatenated feature to a ResNet for frame-level processing. The resulting feature is then passed through a video temporal network [14] to obtain temporal visual representations $f_{v*} \in \mathbb{R}^{T \times D}$. In this way, the visual encoder as a whole not only incorporates cues from frame-level lip landmarks but also leverages temporal modeling to explicitly capture the dynamics of lip movement across video frames.

Our visual encoder can be integrated to state-of-the-art ASD models [5, 15, 25, 26] and can be trained end-to-end by the ASD training objectives described in Equation 1. As we shall see in the experiments, LASER enhances state-of-the-art ASD models across various evaluation protocols.

3.3. Addressing Missing Lip Landmark Tracks

While the proposed LASER achieves strong performance across various evaluation scenarios, we observe that the facial landmark detector does not always return lip landmarks for every face track in videos because of low resolution, occlusion, or extreme angles in the facial frames. For example, on the AVA-ActiveSpeaker dataset [18], the detector fails to predict lip landmarks for approximately 15% of face tracks. At test time, the absence of lip landmarks results in suboptimal visual features, which can negatively impact the model’s performance.

To enable our visual encoder \mathcal{F}_v to effectively handle face tracks that are challenging for landmark detectors, we introduce an auxiliary consistency loss to enforce consistency between the predictions made from LASER-enhanced features and those from standard face track features. Specifically, given a face track $V \in \mathbb{R}^{T \times H \times W}$, we obtain the visual representation $f_v = \mathcal{F}_v(V)$ without lip track encoding and $f_{v*} = \mathcal{F}_v(V, \mathcal{T}(M))$ with lip track encoding, where $\mathcal{T}(M)$ represents the lip landmark encoding. The consistency loss is then defined as the KL-Divergence between the final predictions made with f_v and f_{v*} :

$$\mathcal{L}_{\text{consistency}} = \sum_{j=0}^1 \mathcal{G}(f_v)_j \cdot \log \frac{\mathcal{G}(f_v)_j}{\mathcal{G}(f_{v*})_j} \quad (4)$$

where j denotes the class index of prediction. We apply stop gradient operation on f_{v*} (predictions made with lips track encoding) when computing the consistency loss so that gradients only flow through f_v (predictions without lips track encoding), encouraging the model to match the predictions it makes with lips track encoding. This approach ensures the model learns to make reliable predictions even when mouth landmarks are unavailable at test time.

The final training objective is defined as

$$\mathcal{L} = \mathcal{L}_{\text{asd}} + \lambda_c \mathcal{L}_{\text{consistency}} \quad (5)$$

where \mathcal{L}_{asd} is the default training objective of ASD models [5, 15, 25, 26] from Section 3.1. By enforcing consistent predictions between face tracks with and without

lip track encoding, our model achieves robust performance even on challenging face tracks where facial landmark detection may fail. Notably, as demonstrated in our experiments, this approach allows us to eliminate the reliance on the facial landmark detector altogether, using only face tracks at test time without sacrificing performance.

4. Experiments

In this section, we evaluate the effectiveness of our proposed Lip landmark Assisted Speaker detection for Robustness (LASER) method. We assess its performance on multiple datasets and compare it against baseline models to demonstrate improvements in active speaker detection tasks in different evaluation scenarios. We also ablate our design choices.

4.1. Experimental Setup

4.1.1. Implementation Details

To demonstrate the efficacy of LASER, we implement it with the state-of-the-art ASD model LoCoNet [26]. We closely follow the training details for fair comparison. Specifically, we use batch size of 4 and sample 200 frames per training example. We use Adam [6] as our optimizer with learning rate of 5×10^{-5} that reduces by 0.5% per epoch. Each model is trained with 25 epochs on 4 RTX 2080 GPUs. For ASD training objectives, we follow the LoCoNet [26] setting $\lambda_{av} = 1$, $\lambda_a = 0.4$, and $\lambda_v = 0.4$. Random resizing, cropping, horizontal flipping, and rotations are used as visual data augmentation operations and a randomly selected audio signal from the training set is added as background noise to the target audio [25].

4.1.2. Datasets

We experiment on common Active Speaker Benchmark datasets AVA-ActivateSpeaker [18], Talkies [2] and ASW [12]. AVA-ActivateSpeaker is the current biggest dataset for the Active Speaker Detection task. It consists of 262 videos spanning over 38 hours with over 38,500 tracks and over 3.65 million faces. Talkies [2] is one of the in-the-wild active speaker datasets with more than 799,000 faces detected from over 10,000 unique videos. On average, there are about 2.3 faces per frame which is greater than the average of 1.6 faces per frame of AVA-ActiveSpeaker. ASW [12] is an in-the-wild active speaker dataset along side Talkies. It contains 212 videos from the VoxConverse dataset [4], and consists of a total of 11,551 face tracks spanning over 30.9 hours.

4.1.3. Evaluation Protocols

We use the following evaluation protocols to assess the performance of LASER and baseline methods:

(1) *Evaluation with synchronized audios*: This is the standard evaluation protocol, where both training and test-

Model	AVA	Talkies	ASW
TalkNet [25]	92.3	-	-
EASEE [3]	94.1	86.7	-
MAAS [2]	88.8	79.7	-
LoCoNet [26]	95.2	88.4	88.4
LASER (ours)	95.3	89.0	88.9
LoCoNet w/ CL [10]	95.5	88.3	88.5
LASER + w/ CL (ours)	95.4	89.7	89.5

Table 1. **Evaluation with synchronized audios.** The models are trained on AVA-ActiveSpeaker dataset only and evaluated on AVA, as in-domain evaluation and Talkies and ASW as out-of-domain evaluations. CL denotes contrastive learning.

ing data have synchronized audio and face tracks. We evaluate on both in-domain scenarios (where training and testing data come from the same dataset) and out-of-domain scenarios (where testing data comes from different datasets). We use AVA-ActiveSpeaker as our in-domain datasets and Talkies and ASW as our out-of-domain evaluation datasets and use mAP as the evaluation metric following common practice [18].

(2) *Evaluation with unsynchronized audios:* This protocol simulates a non-speaking scenario by introducing a short delay at the beginning of the audio track in the test data, creating a minor desynchronization with the face tracks. This setup allows us to evaluate the model’s sensitivity to audiovisual synchronization. We use the same dataset partition as (1) and report the average accuracy across all frames.²

4.1.4. Hyperparameter Selection

LASER introduces two key hyperparameters: the number of dense feature maps for lip track encoding, S , and the weight of the consistency loss, λ_c . We set $S = 4$ and $\lambda_c = 1$ for all evaluations. They are determined through a holdout data evaluation using unsynchronized audio where the audio was randomized by reversing the original track. This scenario differs from evaluation protocol (2), which involves a short delay in audio tracks. Our hyperparameter selection process avoids the risk of “tuning on the test set,” ensuring the generalizability of our method.

4.2. Main Results

4.2.1. Evaluation with Synchronized Audios

We first evaluate our LASER with synchronized audios where the model is trained on the training data of AVA-ActiveSpeaker and evaluated on validation set of AVA-ActiveSpeaker, Talkies, and ASW. As shown in Table 1 (top), LASER still improves upon LoCoNet for in-domain

²mAP is not a proper metrics for this scenario because the ground-truth of all example frames are negative (non-speaking).

Layer	Regular Audio	Noise Audio
3D CNN	92.6	86.6
ResNet	95.1	86.7

Table 2. **Ablation study on lip track encoding integration.** Integrating lip track encoding before 3D-CNN layer (i.e, on RGB frames) results in suboptimal performance.

evaluations when the performance is already saturated on AVA. When evaluating on Talkies and ASW whose data distribution is different from AVA, LASER achieves 89.0 and 88.9 mAP respectively.

Recent work [10] also proposes to add an auxiliary contrastive loss to LoCoNet which brings audio-visual embedding pairs closer when they originate from the same video frame, while pushing them apart otherwise. As shown in Table 1 (bottom), while the contrastive loss enhances LoCoNet’s in-domain performance by 0.3 mAP, it offers limited gains in out-of-domain scenarios. Interestingly, when the same contrastive loss is applied to LASER, our method achieves an additional 1.4 and 1.0 mAP improvement on the Talkies and ASW benchmarks, respectively. These results highlight both the effectiveness and general applicability of LASER.

4.2.2. Evaluation with Unsynchronized Audios

We further demonstrate the robustness of LASER by evaluating with unsynchronized audios. We add short delays of 0.2s to 3s at the beginning of the audio track to create non-speaking scenarios and evaluate the model with original the face track and the shifted audio track. As shown in Figure 4, our LASER consistently outperforms LoCoNet by a large margin across different amount of delays in the audio. These results demonstrate the robustness of LASER in response to unsynchronized audios.

4.3. Ablation Studies

We present ablation studies of LASER in this section. For all results in this section, we use the AVA-ActiveSpeaker dataset in both training and testing. As stated before, we select all our hyperparameters based on the performance with noise audio tracks. We include the results for regular audio tracks in this section for reference only.

4.3.1. Integrating Lip Track Encoding to Visual Features

As discussed in Section 3.2, we integrate the aggregated lip track encoding (LTE) into the visual features produced by the 3D-CNN. We compare this approach with integrating LTE directly with the RGB face frames before the 3D-CNN. As shown in Table 2, integrating LTE before the 3D-CNN leads to a significant performance drop. We speculate that this is due to the limited number of channels in the RGB image, where integrating LTE with additional channels may interfere with the feature extraction process of the original

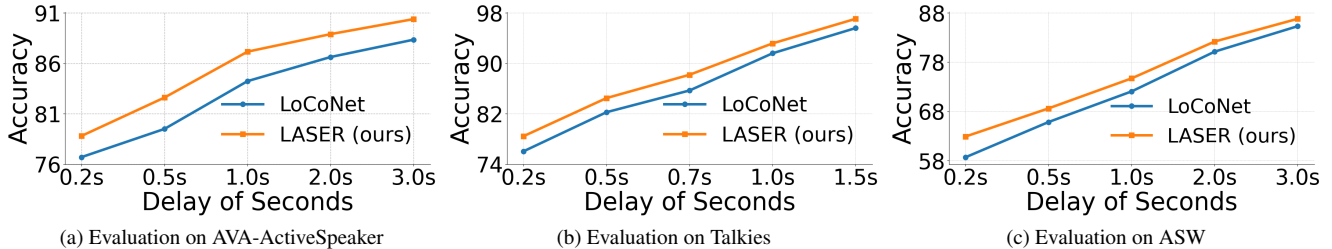


Figure 4. **Evaluation with unsynchronized audios.** We use the same datasets as the evaluation of synchronized audios and report the per-frame accuracy on in-domain datasets (AVA-ActiveSpeaker) and out-of-domain datasets (Talkies and ASW). LASER consistently outperforms LoCoNet [26] under this evaluation protocol.

Consistency Loss	Lip Track Encoding	Regular Audio	Noise Audio
	✓	95.1	86.7
✓	✓	95.3	87.5
✓		95.3	87.5

Table 3. **Ablation study on the consistency loss.** Consistency loss improves the performance on AVA-ActiveSpeaker dataset with approximately 15% videos with missing lips landmark track. Furthermore, with consistency loss, the model achieves similar performance even without lip track encoding, eliminating the dependency of lips track at test time.

face frame. Thus, we opt to integrate LTE into the visual features output by the 3D-CNN.

Stage	# Channels S				
	1	2	4	8	16
1	84.9	84.3	86.9	85.6	84.7
2	84.3	84.7	86.2	83.6	85.0
3	85.5	84.2	83.8	86.1	82.9
4	85.3	86.5	85.1	84.9	82.4

Table 4. **Ablation study on lip track integration with different stages of ResNet.** Setting $S = 4$ and integrating lip track encoding before the first stage of ResNet results in the best performance.

We further investigate integrating LTE to different stages within ResNet. ResNet models have 4 internal stages with different downsampling strides and we investigate the choice of integration before each of the four stages. As shown in Table 4, integrating LTE to features before entering the first stage (i.e., the output feature from 3D-CNN) achieves the overall best performance when evaluated with noise audio tracks and integrating it to subsequent stages within ResNet consistently decreases the performance. Therefore, we choose to integrate LTE to the visual features output by 3D-CNN (i.e., before the first stage of ResNet).

4.3.2. Number of Lip Track Encoding Channels

Recall that we aggregate the initial sparse lip track encodings from $K = 82$ to $S = 4$ dense feature maps through our aggregation process to produce LTE. Here, we examine

Method	λ_c				
	0.2	0.4	0.6	0.8	1.0
Accuracy	85.7	85.9	86.0	85.9	87.5

Table 5. **Ablation study on consistency loss weight.** Setting $\lambda_c = 1$ achieves the best results while decreasing λ_c consistently degrades the performance.

the sensitivity of the choice of S . As shown in Table 4, the choice of S involves a tradeoff: setting S too low overly condenses the information, while setting S too high results in feature maps that remain sparse. Thus, we select $S = 4$, which provides an optimal balance.

4.3.3. Contribution of Consistency Loss

The consistency loss is a key component of LASER designed to address the issue of missing lip track data during test time. Our analysis reveals that the face landmark detector struggles to predict lip landmarks for approximately 15% of the testing face tracks in the AVA-ActiveSpeaker dataset. As shown in Table 3, models trained with the consistency loss achieve a significant improvement when evaluated with both regular and noisy audio inputs. Moreover, when using consistency loss, our models deliver comparable results whether or not lip track encoding is available at test time. This indicates that the visual encoder can successfully capture lip movements through consistency loss, even without the lip track encoding during inference. Consequently, at test time, our model does not rely on the face landmark detector for lip track prediction, which helps reduce the inference latency.

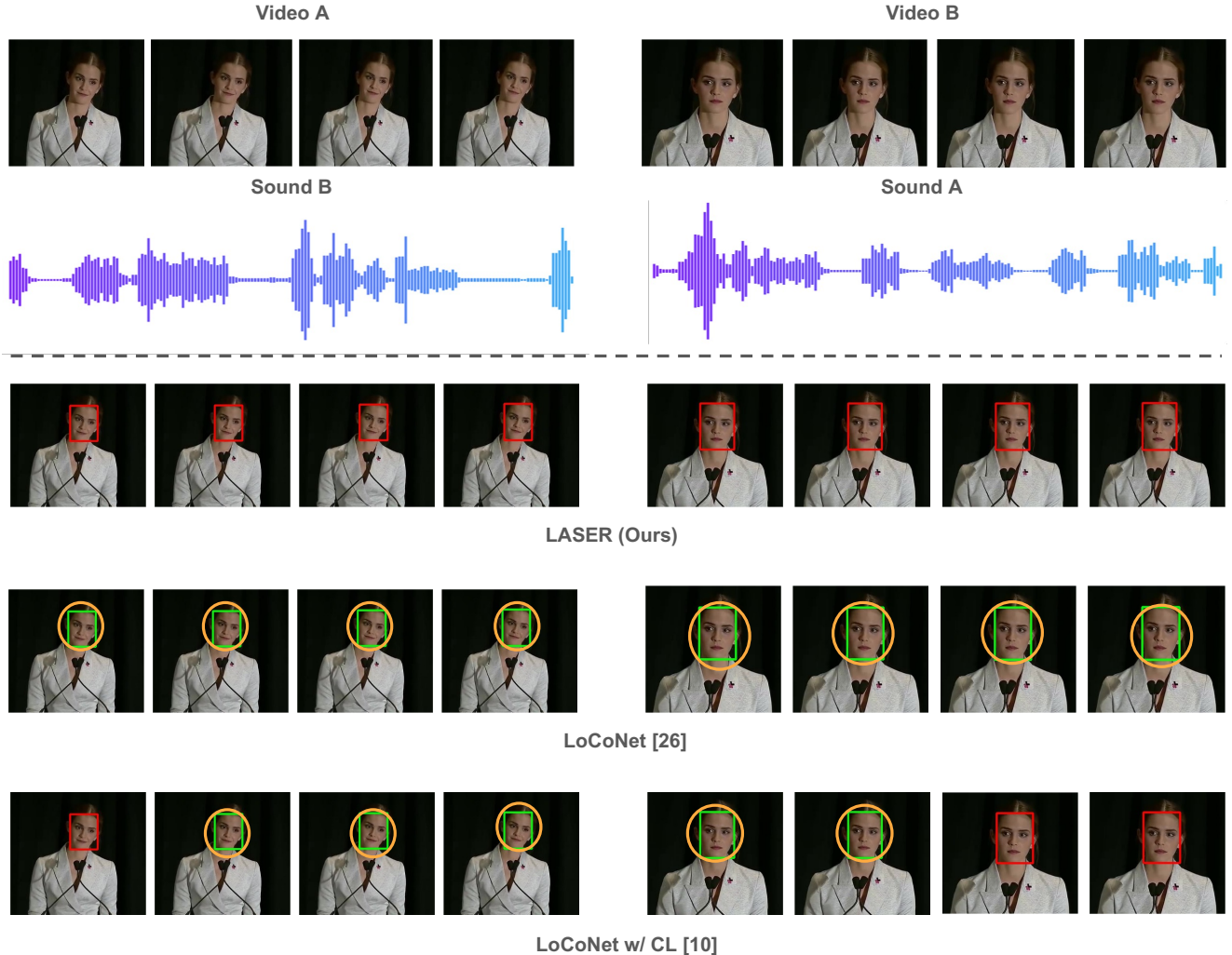


Figure 5. **Qualitative results of LASER, TalkNCE, LoCoNet on two unsynchronized videos.** We create non-speaking scenarios by swapping the audio tracks of two videos where the same person is speaking with similar camera angles. The red box means the model predicts not-speaking. The green box means the model predicts speaking. The yellow circle means the model makes a wrong prediction.

4.3.4. Weight of Consistency Loss

We also study the sensitivity of the weight of consistency loss λ_c where we range the value from 0.2 to 1.0. As shown in Table 5, $\lambda_c = 1$ achieves the best performance whereas decreasing the loss weight consistently hurts the model performance. Thus, we set $\lambda_c = 1$ in all of our experiments.

4.4. Qualitative Results

We provide qualitative comparisons of active speaker detection with real-world videos. Specifically, we collect two video clips with the same person speaking from the same camera angles yet different content in the speech. We then reverse the audio track of the two video clips to create unsynchronization between face tracks and audio tracks.

As shown in Figure 5, the baseline LoCoNet method experiences challenges when predicting non-speaking in

such a challenging scenario whereas our LASER succeeds to make correct predictions in this scenario. The results demonstrate that our LASER is more robust on challenging real-world scenarios.

5. Conclusion

In this work, we introduced LASER for active speaker detection. LASER stands apart from existing methods by explicitly guiding the model to focus on lip landmarks, rather than other raw pixel based facial expressions, enhancing the model’s ability to accurately detect active speakers and improving its sensitivity to audiovisual synchronization. Both quantitative and qualitative results demonstrate that LASER delivers stronger performance compared to the state-of-the-art, especially when visual frames and audio tracks are not synchronized, and exhibits more robust results in real-world video scenarios.

References

- [1] Juan León Alcázar, Fabian Caba, Long Mai, Federico Perazzi, Joon-Young Lee, Pablo Arbeláez, and Bernard Ghanem. Active speakers in context. In *Proceedings of the IEEE/CVF conference on computer vision and pattern recognition*, pages 12465–12474, 2020. 1, 2
- [2] Juan León Alcázar, Fabian Caba, Ali K Thabet, and Bernard Ghanem. Maas: Multi-modal assignation for active speaker detection. In *Proceedings of the IEEE/CVF International Conference on Computer Vision*, pages 265–274, 2021. 1, 2, 5, 6
- [3] Juan León Alcázar, Moritz Cordes, Chen Zhao, and Bernard Ghanem. End-to-end active speaker detection. In *European Conference on Computer Vision*, pages 126–143. Springer, 2022. 6
- [4] Joon Son Chung, Jaesung Huh, Arsha Nagrani, Triantafyllos Afouras, and Andrew Zisserman. Spot the conversation: Speaker diarisation in the wild. In *Interspeech 2020*. ISCA, 2020. 5
- [5] Gourav Datta, Tyler Etchart, Vivek Yadav, Varsha Hedau, Pradeep Natarajan, and Shih-Fu Chang. Asd-transformer: Efficient active speaker detection using self and multimodal transformers. In *ICASSP 2022-2022 IEEE International Conference on Acoustics, Speech and Signal Processing (ICASSP)*, pages 4568–4572. IEEE, 2022. 1, 2, 3, 5
- [6] P Kingma Diederik. Adam: A method for stochastic optimization. *arXiv preprint arXiv:1412.6980*, 2014. 5
- [7] Mark Everingham, Josef Sivic, and Andrew Zisserman. Taking the bite out of automated naming of characters in tv video. *Image and Vision Computing*, 27(5):545–559, 2009. 2
- [8] Zhiqi Ge, Hongzhe Huang, Mingze Zhou, Juncheng Li, Guoming Wang, Siliang Tang, and Yueting Zhuang. Worldgpt: Empowering llm as multimodal world model. In *Proceedings of the 32nd ACM International Conference on Multimedia*, pages 7346–7355, 2024. 1
- [9] Kaiming He, Xiangyu Zhang, Shaoqing Ren, and Jian Sun. Deep residual learning for image recognition. In *Proceedings of the IEEE conference on computer vision and pattern recognition*, pages 770–778, 2016. 4
- [10] Chaeyoung Jung, Suyeon Lee, Kihyun Nam, Kyeongha Rho, You Jin Kim, Youngjoon Jang, and Joon Son Chung. Talknce: Improving active speaker detection with talk-aware contrastive learning. In *ICASSP 2024-2024 IEEE International Conference on Acoustics, Speech and Signal Processing (ICASSP)*, pages 8391–8395. IEEE, 2024. 1, 2, 3, 6
- [11] Soo-Han Kang and Ji-Hyeong Han. Video captioning based on both egocentric and exocentric views of robot vision for human-robot interaction. *International Journal of Social Robotics*, 15(4):631–641, 2023. 1
- [12] You Jin Kim, Hee-Soo Heo, Soyeon Choe, Soo-Whan Chung, Yoohwan Kwon, Bong-Jin Lee, Youngki Kwon, and Joon Son Chung. Look who’s talking: Active speaker detection in the wild. *arXiv preprint arXiv:2108.07640*, 2021. 5
- [13] Okan Köpüklü, Maja Taseska, and Gerhard Rigoll. How to design a three-stage architecture for audio-visual active speaker detection in the wild. In *Proceedings of the IEEE/CVF international conference on computer vision*, pages 1193–1203, 2021. 2
- [14] Colin Lea, Rene Vidal, Austin Reiter, and Gregory D Hager. Temporal convolutional networks: A unified approach to action segmentation. In *Computer Vision—ECCV 2016 Workshops: Amsterdam, The Netherlands, October 8-10 and 15-16, 2016, Proceedings, Part III 14*, pages 47–54. Springer, 2016. 4, 5
- [15] Junhua Liao, Haihan Duan, Kanghui Feng, Wanbing Zhao, Yanbing Yang, and Liangyin Chen. A light weight model for active speaker detection. In *Proceedings of the IEEE/CVF Conference on Computer Vision and Pattern Recognition*, pages 22932–22941, 2023. 1, 2, 3, 5
- [16] Camillo Lugaresi, Jiuqiang Tang, Hadon Nash, Chris McClanahan, Esha Uboweja, Michael Hays, Fan Zhang, Chuo-Ling Chang, Ming Guang Yong, Juhyun Lee, et al. Mediapipe: A framework for building perception pipelines. *arXiv preprint arXiv:1906.08172*, 2019. 2, 4
- [17] Hyojin Park, Christoph Kayser, Gregor Thut, and Joachim Gross. Lip movements entrain the observers’ low-frequency brain oscillations to facilitate speech intelligibility. *eLife*, 5, 2016. 1
- [18] Joseph Roth, Sourish Chaudhuri, Ondrej Klejch, Radhika Marvin, Andrew Gallagher, Liat Kaver, Sharadh Ramaswamy, Arkadiusz Stopczynski, Cordelia Schmid, Zhonghua Xi, et al. Ava active speaker: An audio-visual dataset for active speaker detection. In *ICASSP 2020-2020 IEEE International Conference on Acoustics, Speech and Signal Processing (ICASSP)*, pages 4492–4496. IEEE, 2020. 2, 3, 5, 6
- [19] Sourya Roy, Kyle Min, Subarna Tripathi, Tanaya Guha, and Somdeb Majumdar. Learning spatial-temporal graphs for active speaker detection. *arXiv preprint arXiv:2112.01479*, 2021. 1, 2
- [20] Kate Saenko, Karen Livescu, Michael Siracusa, Kevin Wilson, James Glass, and Trevor Darrell. Visual speech recognition with loosely synchronized feature streams. In *Tenth IEEE International Conference on Computer Vision (ICCV’05) Volume 1*, pages 1424–1431. IEEE, 2005. 2
- [21] Ramprasaath R. Selvaraju, Michael Cogswell, Abhishek Das, Ramakrishna Vedantam, Devi Parikh, and Dhruv Batra. Grad-cam: Visual explanations from deep networks via gradient-based localization. *International Journal of Computer Vision*, 128(2):336–359, 2019. 3
- [22] Thomas B Sheridan. Human–robot interaction: status and challenges. *Human factors*, 58(4):525–532, 2016. 1
- [23] Fangxun Shu, Lei Zhang, Hao Jiang, and Cihang Xie. Audio-visual llm for video understanding. *arXiv preprint arXiv:2312.06720*, 2023. 1
- [24] Gabriel Skantze. Turn-taking in conversational systems and human-robot interaction: a review. *Computer Speech & Language*, 67:101178, 2021. 1
- [25] Ruijie Tao, Zexu Pan, Rohan Kumar Das, Xinyuan Qian, Mike Zheng Shou, and Haizhou Li. Is someone speaking?

exploring long-term temporal features for audio-visual active speaker detection. In *Proceedings of the 29th ACM international conference on multimedia*, pages 3927–3935, 2021. [1](#), [2](#), [3](#), [4](#), [5](#), [6](#)

- [26] Xizi Wang, Feng Cheng, and Gedas Bertasius. Loconet: Long-short context network for active speaker detection. In *Proceedings of the IEEE/CVF Conference on Computer Vision and Pattern Recognition*, pages 18462–18472, 2024. [1](#), [2](#), [3](#), [4](#), [5](#), [6](#), [7](#)
- [27] Shengqiong Wu, Hao Fei, Leigang Qu, Wei Ji, and Tat-Seng Chua. Next-gpt: Any-to-any multimodal llm. *arXiv preprint arXiv:2309.05519*, 2023. [1](#)